

Evidence for universal four-body states tied to an Efimov trimer

F. Ferlaino,¹ S. Knoop,¹ M. Berninger,¹ W. Harm,¹ J. P. D’Incao,^{2,3} H.-C. Nägerl,¹ and R. Grimm^{1,2}

¹Institut für Experimentalphysik and Zentrum für Quantenphysik, Universität Innsbruck, 6020 Innsbruck, Austria

²Institut für Quantenoptik und Quanteninformation, Österreichische Akademie der Wissenschaften, 6020 Innsbruck, Austria

³JILA, University of Colorado and NIST, Boulder, Colorado 80309-0440, USA

(Dated: March 19, 2019)

We report on the measurement of four-body recombination rate coefficients in an atomic gas. Our results obtained with an ultracold sample of cesium atoms at negative scattering lengths show a resonant enhancement of losses and provide strong evidence for the existence of a pair of four-body states, which is strictly connected to Efimov trimers via universal relations. Our findings confirm recent theoretical predictions and demonstrate the enrichment of the Efimov scenario when a fourth particle is added to the generic three-body problem.

PACS numbers: 03.75.-b, 34.50.Cx, 67.85.-d, 21.45.-v

Few-body physics produces bizarre and counterintuitive phenomena, with the Efimov effect representing the major paradigm of the field [1]. Early in the 1970s, Efimov found a solution to the quantum three-body problem, predicting the existence of an infinite series of universal weakly bound three-body states. Surprisingly, these Efimov trimers can even exist under conditions where a weakly bound dimer state is absent [2, 3, 4]. An essential prerequisite for the Efimov effect is a large two-body scattering length a , far exceeding the characteristic range of the interaction potential. Ultracold atomic systems with tunable interactions [5] have opened up unprecedented possibilities to explore such few-body quantum systems under well controllable experimental conditions. In particular, a can be made much larger than the van der Waals length r_{vdW} [6], the range of the interatomic interaction. This separation of length scales ($|a| \gg r_{\text{vdW}}$) is at the heart of the universal properties of Efimov states [4].

In the last few years, signatures of Efimov states have been observed in ultracold atomic and molecular gases of cesium atoms [7, 8], and recently in three-component Fermi gases of ^6Li [9, 10], in a Bose gas of ^{39}K atoms [11], and in mixtures of ^{41}K and ^{87}Rb atoms [12]. In all these experiments, Efimov states manifest themselves as resonantly enhanced losses, either in atomic three-body recombination or in atom-dimer relaxation processes. The recent observations highlight the universal character of Efimov states, and they also point to a rich playground for future experiments.

As a next step in complexity, a system of four identical bosons with resonant two-body interaction challenges our understanding of few-body physics. The fundamental questions concern the extension of the concept of universality to such a system and the understanding of its relation to the well-understood Efimov scenario [4]. Accordingly, the four-body problem has been attracting increasing interest both in theory [14, 15, 16, 17, 18, 19] and experiment [13]. An interesting question under debate is the possible close connection between universal three- and four-body states [14, 15, 16, 17, 19]. In this context, Hammer and Platter predicted the four-body system to support universal tetramer states in close connection with Efimov trimers [17].

Recently, von Stecher, D’Incao, and Greene presented key

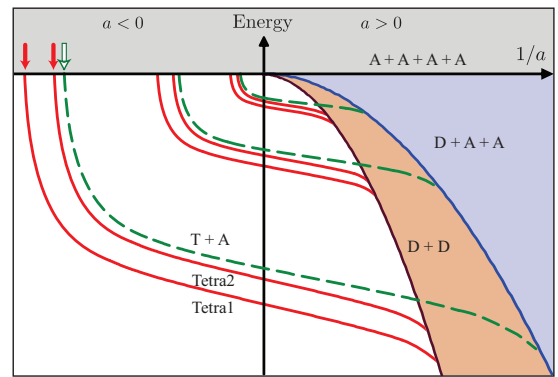


FIG. 1: (color online) Extended Efimov scenario describing a universal system of four identical bosons; Energies are plotted as a function of the inverse scattering length. The red solid lines illustrate the pairs of universal tetramer states (Tetra1 and Tetra2) associated with each Efimov trimer (T). For illustrative purposes, we have artificially reduced the universal Efimov scaling factor from 22.7 to about 2. The shaded regions indicate the scattering continuum associated with the relevant dissociation threshold. The four-body threshold is at zero energy and refers to four free atoms (A+A+A+A). In the $a > 0$ region, the dimer-atom-atom threshold (D+A+A) and the dimer-dimer threshold (D+D) are also depicted. The weakly bound dimer, only existing for $a \gg r_{\text{vdW}} > 0$, has universal halo character and its binding energy is given by $\hbar^2/(ma^2)$ [2, 13]. The open arrow marks the intersection of the first Efimov trimer (T) with the atomic threshold, while the filled arrows indicate the corresponding locations of the two universal tetramer states.

predictions for universal four-body states [19]. For each Efimov trimer, they demonstrate the existence of a pair of universal tetramer states; the latter states are tied to the corresponding trimer through simple universal relations that do not invoke any four-body parameter [16, 17, 19]. The authors of Ref. [19] suggest resonantly enhanced four-body recombination in an atomic gas as a probe for such universal tetramer states. They also find hints on the existence of one of the predicted four-body resonances by reinterpreting our earlier recombination measurements on ^{133}Cs atoms at large negative scattering lengths [7]. In this Letter, we present new mea-

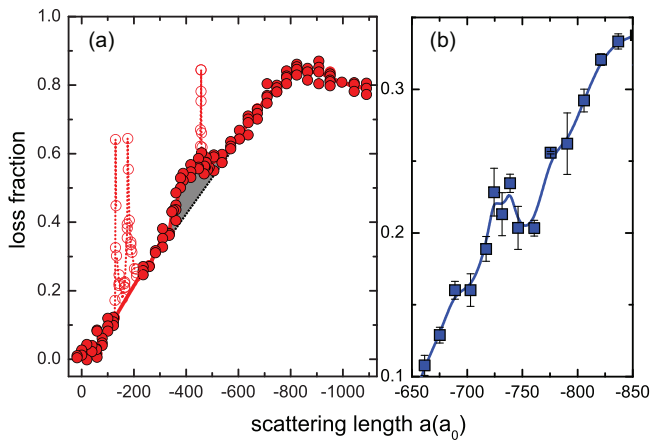


FIG. 2: (color online) Loss fraction in an ultracold sample of Cs atoms at (a) about 50 nK after a storage time of 250 ms and (b) at about 30 nK after a storage time of 8 ms. In (a) the broad maximum at about $-870a_0$ is caused by a triatomic Efimov resonance [7] and the shaded area highlights the resonant loss enhancement that we attribute to the four-body state Tetra1; see text. The three very narrow loss resonances (open circles) are caused by known g -wave Feshbach resonances [20], which are irrelevant in the present context. In (b) the loss enhancement at around $-730a_0$ is caused by the state Tetra2. The solid lines are spline interpolations guiding the eye.

measurements on the Cs system dedicated to four-body recombination in the particular region of interest near a triatomic Efimov resonance. Our results clearly verify the key predictions of Ref. [19]. We observe two loss resonances as a signature of the predicted tetramer pair and we find strong evidence for the four-body nature of the underlying recombination process.

The four-body extended Efimov scenario [17, 19] is schematically illustrated in Fig. 1, where the tetramer states (Tetra1 and Tetra2) and the relevant thresholds are depicted as a function of the inverse scattering length $1/a$. Within the four-body scenario, the Efimov trimers (T) are associated with trimer-atom thresholds (T+A, dashed lines). The pair of universal tetramer states (solid lines) lies below the corresponding T+A threshold. The four-body breakup threshold (A+A+A+A) defines zero energy and refers to the continuum of four free atoms. For completeness, we also show the $a > 0$ region. Here, the picture is even richer because of the presence of the weakly bound dimer state, which leads to the dimer-atom-atom threshold (D+A+A) and the dimer-dimer threshold (D+D). In the four-body scenario, the tetramer states emerge at the atomic threshold for $a < 0$ and connect to the D+D threshold for $a > 0$.

The Efimov trimer intersects the atomic threshold at $a = a_T^*$, which leads to the observed triatomic resonance [7]. The corresponding tetramer states are predicted [19] to intersect the atomic threshold at scattering length values

$$a_{\text{Tetra1}}^* \approx 0.43 a_T^* \quad \text{and} \quad a_{\text{Tetra2}}^* \approx 0.9 a_T^*. \quad (1)$$

These universal relations, linking three- and four-body resonances, express the fact that no additional parameter, namely the so-called four-body parameter, is needed to describe the

system behavior. In contrast to the connection between universal two- and three-body systems, where a three-body parameter is required to locate the trimer states, the universal properties of the four-body system are thus directly related to the corresponding three-body subsystem.

In analogy to the well-established fact that Efimov trimers lead to loss resonances in an atomic gas [7, 21], universal four-body states can also be expected to manifest themselves in a resonant increase of atomic losses [19]. Resonant coupling between four colliding atoms and a tetramer state ($a \simeq a_{\text{Tetra}}^* < 0$) drastically enhances four-body recombination to lower lying channels. Possible decay channels are trimer-atom, dimer-dimer, and dimer-atom-atom channels [18]. In each of these recombination processes, we expect all the particles to rapidly escape from the trap, as the kinetic energy gained usually exceeds the trap depth.

We prepare an ultracold optically trapped atomic sample in the lowest hyperfine sublevel ($F = 3, m_F = 3$) [22], as described in Ref. [13]. By varying the magnetic field between 6 and 17 G, the scattering length a can be tuned from -1100 to $0 a_0$ [23], where a_0 is Bohr's radius. For presenting our experimental data in the following, we convert the applied magnetic field into a using the fit formula of Ref. [7]. After several cooling and trapping stages [23], the atoms are loaded into an optical trap, formed by crossing two infrared laser beams [13]. The trap frequencies in the three spatial directions are about $(\omega_x, \omega_y, \omega_z) = 2\pi \times (10, 46, 65)$ Hz. Similar to [23], we support the optical trap by employing a magnetic levitation field acting against gravity. Evaporative cooling in the levitated trap is stopped just before the onset of Bose-Einstein condensation in order to avoid implosion of the gas. For our typical temperature of 50 nK, we obtain about 8×10^4 non-condensed atoms with a peak density of about $7 \times 10^{12} \text{ cm}^{-3}$.

In a first set of experiments, we study the atomic losses after a fixed storage time in the optical trap for variable scattering length in the $a < 0$ region. In Fig. 2(a), we show the measured atomic loss fraction after a storage time of 250 ms; here we present all individual measurements to give an impression of the scatter of our data. In Fig. 2(b), we reduce the storage time to 8 ms, in order to prevent strong three-body losses from masking four-body processes. Here the plot shows the average values resulting from five individual measurements for a given a together with their statistical errors.

The observed losses displayed in Fig. 2 incorporate both three- and four-body processes. Three-body losses give rise to a background loss following a general a^4 -scaling behavior [21, 24, 25] with a triatomic Efimov resonance emerging on top of it [4]. At 50 nK, the resonance occurs at $a_T^* = -870(10)a_0$, as previously observed in [7, 26]; this is consistent with the large losses shown in Fig. 2(a). In addition to the expected behavior of the three-body subsystem, we clearly observe two maxima, one located at about $-410a_0$ [Fig. 2(a)] and one at about $-730a_0$ [Fig. 2(b)]. We interpret these two resonant loss features as the predicted pair of four-body resonances [19]. For the resonance positions we find $a_{\text{Tetra1}}^*/a_T^* \simeq 0.47$ and $a_{\text{Tetra2}}^*/a_T^* \simeq 0.84$, which are remark-

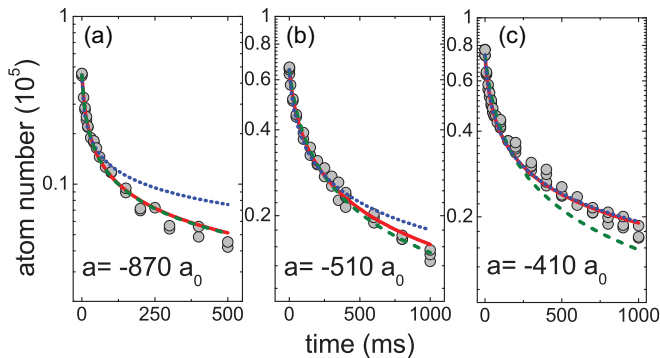


FIG. 3: (color online) Time evolution of the number of atoms in an optically trapped sample. The solid lines are the fit to the data based on the full numerical solution of Eq. (2). The dashed and dotted lines correspond to a pure three-body and pure four-body decay, respectively (see text). (a) For dominant three-body collisions ($a = -870a_0$), (b) an intermediate situation ($a = -510a_0$), and (c) dominant four-body collisions ($a = -410a_0$).

ably close to the predicted positions of Eq. (1).

In a second set of experiments, we study the time-dependence of the atomic decay in the optical trap. Here we focus on the region around the resonance at $a_{\text{Tetra1}}^* \simeq -410a_0$, where the three-body losses are comparatively weak. Representative loss measurements for three different values of a are shown in Fig. 3.

The observed decay can be fully attributed to three-body and four-body recombination collisions. This is due to the fact that inelastic two-body collisions of atoms in the lowest Zeeman sub-level are energetically suppressed, and one-body losses, such as background collisions or light-induced losses, can be completely neglected under our experimental conditions. The corresponding differential equation for the decaying atom number reads as

$$\dot{N}/N = -L_3\langle n^2 \rangle - L_4\langle n^3 \rangle, \quad (2)$$

where L_3 and L_4 denote the three- and the four-body recombination rate coefficient, respectively. The average density is calculated by integrating the density over the volume $\langle n^2 \rangle = (1/N) \int n^3 d^3\mathbf{r}$ and $\langle n^3 \rangle = (1/N) \int n^4 d^3\mathbf{r}$. By considering a thermal density distribution of gaussian shape in the three-dimensional harmonic trap, we obtain $\langle n^2 \rangle = n_p^2/\sqrt{27}$ and $\langle n^3 \rangle = n_p^3/8$, with $n_p = \sqrt{8}N[m\bar{\omega}^2/(4\pi k_B T)]^{3/2}$ the peak density. Here, m is the atomic mass, T the temperature, and $\bar{\omega} = (\omega_x \omega_y \omega_z)^{1/3}$ the mean trap frequency. We determine the trap frequencies and the temperature by sloshing mode and time-of-flight measurements, respectively.

In general Eq. (2) is not analytically solvable. An analytic solution can be found in the limit of either pure three-body losses or pure four-body losses. Therefore we fit our decay curves with a numerical solution of Eq. (2), keeping both L_3 and L_4 as free parameters. Note that we have not included anti-evaporation heating [25] in our model because we do not observe the corresponding temperature increase in our experiments. We believe that, for the fast decay observed here, the

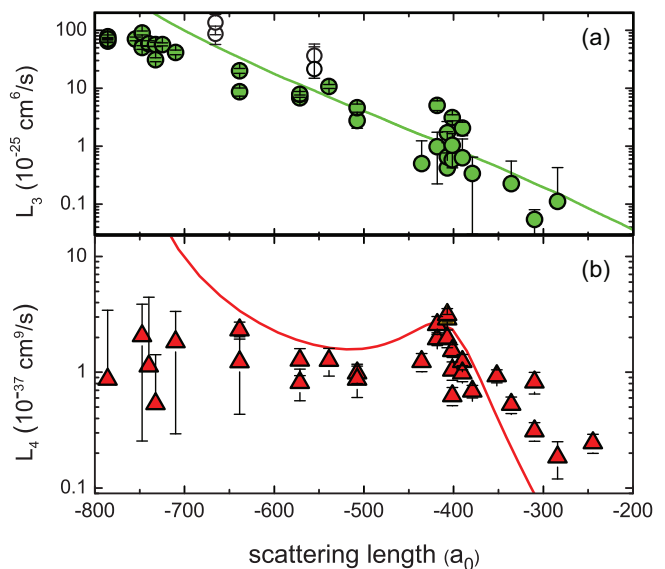


FIG. 4: (color online) Loss rate coefficient for (a) three- and (b) four-body recombination as a function of the scattering length a . The measurements are taken at temperatures of about 40 nK. The values are obtained by fitting the numerical solution of Eq. (2) to the decay curve. The error bars on L_3 and L_4 are the statistical uncertainties from the fit evaluated with a resampling method [27]. The open circles in (a) refer to previous data at 250 nK [7]. The solid curves result from the theoretical model of Refs. [19, 28].

sample may not have enough time to thermalize.

Our experimental data clearly reveal a qualitative change of the decay curves when a is tuned between a_{T1}^* and a_{Tetra1}^* . Fig. 3(a) shows that for $a \approx a_{\text{T1}}^*$ the loss is dominated by three-body recombination; here the full numerical fitting curve follows the pure three-body solution. A different situation is found at $-410a_0$; see Fig. 3(c). Here a pure three-body analysis cannot properly describe the observed behavior and the full numerical solution reveals a predominant four-body character. In intermediate situations, for which an example is shown in Fig. 3(b), both three- and four-body processes significantly contribute to the observed decay.

From the decay curves taken at different values of a we determine L_3 and L_4 ; the results are shown in Fig. 4. The three-body contribution L_3 follows previously observed behavior [7], as dictated by the a^4 -scaling in combination with the Efimov effect.

Our major result is shown in Fig. 4(b), where we plot the rate coefficient L_4 . Our data provide the first available quantitative information on L_4 , establishing the role of four-body collisions in ultracold gases. For $|a| < |a_{\text{Tetra1}}^*|$, where no universal tetramer states exist, the four-body losses are typically very weak. Here, we measure $L_4 \simeq 0.2 \times 10^{-37} \text{cm}^9/\text{s}$. With increasing $|a|$, the system undergoes a significant change in its behavior, with four-body collisions dominating the atomic decay; see Fig. 3(c). We observe a sharp increase of L_4 , which reaches its maximum value at $a = -412(2)a_0$. This observation is another strong piece of evidence for the predicted uni-

versal four-body state at a_{Tetra}^* [19]. To directly estimate the relative contributions of three- and four-body recombination, one can compare L_3 with $n_0 L_4$, where $n_0 \simeq 1.0 \times 10^{13} \text{ cm}^{-3}$ is the initial peak density at 40 nK. At resonance, $n_0 L_4$ exceeds L_3 by more than one order of magnitude, with $L_3 = 0.7 \times 10^{-25} \text{ cm}^6/\text{s}$ and $n_0 L_4 = 3 \times 10^{-24} \text{ cm}^6/\text{s}$. With further increasing $|a|$, L_4 decreases and L_3 increases such that $L_3 > n_0 L_4$. For $|a| > 700a_0$, the three-body losses are so strong that the fit does no longer provide precise values for L_4 , as seen by the larger scatter and uncertainty of our data points.

Figure 4 also includes the theoretical predictions for L_3 and L_4 at 40 nK and demonstrates a remarkable qualitative agreement with our experimental results. The theoretical approach utilizes a solution of the four-body problem in the hyperspherical adiabatic representation [19]; the derivation and associated calculations of L_4 , adapted from [28], provide the first quantitative description of the four-body recombination rate. The calculations only require to fix the position of the triatomic Efimov resonance as determined in the previous experiment at 10 nK of Ref. [7]. The difference in the width and the amplitude of the four-body resonance between experimental and theoretical data may be explained by different coupling to possible decay channels.

Our work leads to important conclusions related to the concept of universality with increasing complexity. The observation of the universal ratios linking three- and four-body states confirms that a four-body parameter is not required. Universal four-body states emerge as a genuine consequence of the three-body Efimov spectrum. This also provides a novel way to test Efimov physics. The Efimovian character of a three-body resonance can be verified by observing the universal tetramer resonances tied to it, without the necessity to explore the full geometric scaling of Efimov physics by changing the scattering length by orders of magnitude.

While our present work has focussed on four-body phenomena at negative scattering length, a further exciting step will be the exploration of the entire four-body spectrum. For positive scattering lengths, the spectrum becomes richer and new phenomena can be expected such as resonant interactions between four-body states and two-dimer states. In this way, experiments on few-body phenomena in ultracold atoms will keep on challenging our understanding of the universal physics of a few resonantly interacting particles.

We are aware of related results in ^{39}K , in which enhanced losses near a Feshbach resonance may be interpreted as a four-body resonance [29].

We acknowledge C. Greene and J. von Stecher for stimulating discussions and for sharing their theoretical curves (Fig. 4) with us. We acknowledge support by the Austrian Science Fund (FWF) within SFB 15 (project part 16). F.F. is supported within the Lise Meitner program of the FWF.

- [2] A. S. Jensen, K. Riisager, D. V. Fedorov, and E. Garrido, *Rev. Mod. Phys.* **76**, 215 (2004).
- [3] T. Köhler, K. Góral, and P. S. Julienne, *Rev. Mod. Phys.* **78**, 1311 (2006).
- [4] E. Braaten and H.-W. Hammer, *Phys. Rep.* **428**, 259 (2006).
- [5] C. Chin, R. Grimm, P. Julienne, and E. Tiesinga, submitted to *Rev. Mod. Phys.* (2008).
- [6] The van der Waals length is defined as $r_{\text{vdW}} = \frac{1}{2}(mC_6/\hbar^2)^{1/4}$, where C_6 is the van der Waals dispersion coefficient [3]. For Cs, $r_{\text{vdW}} = 100a_0$.
- [7] T. Kraemer, M. Mark, P. Waldburger, J. G. Danzl, C. Chin, B. Engeser, A. D. Lange, K. Pilch, A. Jaakkola, H.-C. Nägerl, and R. Grimm, *Nature* **440**, 315 (2006).
- [8] S. Knoop, F. Ferlaino, M. Mark, M. Berninger, H. Schöbel, H.-C. Nägerl, and R. Grimm, *Nat. Phys.* **5**, 227 (2009).
- [9] T. B. Ottenstein, T. Lompe, M. Kohnen, A. N. Wenz, and S. Jochim, *Phys. Rev. Lett.* **101**, 203202 (2008).
- [10] J. H. Huckans, J. R. Williams, E. L. Hazlett, R. W. Stites, and K. M. O'Hara, arXiv:0810.3288 (2008).
- [11] M. Zaccanti, G. Modugno, C. D'Errico, M. Fattori, G. Roati, and M. Inguscio, talk at DAMOP-2008, 27-31 May 2008, State College, Pennsylvania, USA.
- [12] G. Barontini, C. Weber, F. Rabatti, J. Catani, G. Thalhammer, M. Inguscio, and F. Minardi, arXiv:0901.4584 (2009).
- [13] F. Ferlaino, S. Knoop, M. Mark, M. Berninger, H. Schöbel, H.-C. Nägerl, and R. Grimm, *Phys. Rev. Lett.* **101**, 023201 (2008).
- [14] L. Platter, H. Hammer, and U. Meißner, *Phys. Rev. A* **70**, 052101 (2004).
- [15] M. Yamashita, L. Tomio, A. Delfino, and T. Frederico, *Europhys. Lett.* **75**, 555 (2006).
- [16] G. J. Hanna and D. Blume, *Phys. Rev. A* **74**, 063604 (2006).
- [17] H. Hammer and L. Platter, *Eur. Phys. J. A* **32**, 113 (2007).
- [18] Y. Wang and B. D. Esry, arXiv:0809.3779 (2008).
- [19] J. von Stecher, J. P. D'Incao, and C. H. Greene, arXiv:0810.3876 (2008).
- [20] C. Chin, V. Vuletić, A. J. Kerman, S. Chu, E. Tiesinga, P. J. Leo, and C. J. Williams, *Phys. Rev. A* **70**, 032701 (2004).
- [21] B. D. Esry, C. H. Greene, and J. P. Burke, *Phys. Rev. Lett.* **83**, 1751 (1999).
- [22] F and m_F indicate the hyperfine and projection quantum number, respectively.
- [23] T. Weber, J. Herbig, M. Mark, H.-C. Nägerl, and R. Grimm, *Science* **299**, 232 (2003).
- [24] P. O. Fedichev, M. W. Reynolds, and G. V. Shlyapnikov, *Phys. Rev. Lett.* **77**, 2921 (1996).
- [25] T. Weber, J. Herbig, M. Mark, H.-C. Nägerl, and R. Grimm, *Phys. Rev. Lett.* **91**, 123201 (2003).
- [26] H.-C. Nägerl, T. Kraemer, M. Mark, P. Waldburger, J. G. Danzl, B. Engeser, A. D. Lange, K. Pilch, A. Jaakkola, C. Chin, and R. Grimm, *Atomic Physics 20 AIP Conf. Proc.* **869**, 269 (2006), cond-mat/0611629.
- [27] P. H. Westfall and S. S. Young, eds., *Resampling-Based Multiple Testing* (John Wiley and Sons, New York, 1993).
- [28] N. P. Mehta, S. T. Rittenhouse, J. von Stecher, J. P. D'Incao, and C. H. Greene, *A general theoretical description of N-body recombination*, unpublished (2009).
- [29] M. Zaccanti, private communication (2009).

[1] V. Efimov, *Phys. Lett. B* **33**, 563 (1970).